iJRASET
International Journal For Research in Applied Science and Engineering Technology

INTERNATIONAL JOURNAL FOR RESEARCH

IN APPLIED SCIENCE & ENGINEERING TECHNOLOGY

Volume: 11 **Issue:** XII **Month of publication:** December 2023

DOI: https://doi.org/10.22214/ijraset.2023.57710

www.ijraset.com

Call: 08813907089 | E-mail ID: ijraset@gmail.com

International Journal for Research in Applied Science & Engineering Technology (IJRASET)
ISSN: 2321-9653; IC Value: 45.98; SJ Impact Factor: 7.538
Volume 11 Issue XII Dec 2023- Available at www.ijraset.com

Role of Annealing Temperature on Improving the Hydrogen Storage Capacity of Copper Nano-Particles Decorated Carbon Nano Materials Synthesized from Sugarcane Bagasse

Bholanath T. Mukherjee[1], Manoj D. Basutkar[2], Suyash S. Prasad[3]
[1, 2, 3]*DSPM'S K.V. Pendharkar College, Dombivli, Maharashtra, India*

Abstract: ***This study focuses on improving hydrogen storage capacity of Carbon Nano Materials (CNMs) by investigating the role of annealing temperature for the synthesis of Copper Nano-Particles (CuNPs) decorated CNMs synthesized from sugarcane bagasse (SCB). SCB was pyrolyzed at around 750°C in an inert medium. Pyrolyzed carbon thus obtained was activated by alkali. These activated carbons were then decorated with CuNPs by annealing at different temperatures in CO_2 atmosphere. The CNMs thus synthesized were characterized using XRD and Raman spectroscopic analysis to elucidate the structural intervention with particle size and defects respectively, while EDAX and ICP-AES were utilized to quantify the amount of copper deposited. SEM analysis depicts the porous morphology being decorated with spherical copper nanoparticles. Hydrogen Storage capacity was explored using Sievert's apparatus. Pore volumes of CNMs synthesized at different annealing temperature were determined from adsorption isotherm co-relating it with hydrogen adsorption observation from Sievert's apparatus for evaluating better hydrogen storage.***

Keywords: Sugarcane Bagasse (SCB), Carbon Nano Material (CNM), Copper Nano-Particles (CuNPs), Hydrogen Adsorption Capacity, Sievert's apparatus, Hydrogen Storage

I. INTRODUCTION

Non-renewable fossil fuel source like Petroleum and petrochemicals are depleting day by day generating hazardous emission that adversely affect environment [1]. Multitude of research work is under way to generate sustainable and environment friendly fuel sources that can be generated at competitive costs to current petroleum sources [2] [3].

Hydrogen being one of the most abundant elements on the planet proves to be a sustainable and promising alternative fuel, generating significant energy and water as an emission products [4]. Hydrogen has a unique capability of either driving the IC engines, thus utilising the existing established machinery to be used with minor modifications [5], or being able to generate electricity through the hydrogen fuel cells [6], both generating energy in most desired form without generating hazardous wastes [7]. This makes hydrogen a safe, versatile, and convenient fuel source [8].

The bottle neck in utilizing hydrogen as a fuel lies in its storage [9]. Hydrogen being gas, it must be compressed and stored under pressure cylinders to achieve desired energy density. It is unsafe to use high pressure containers for utilising hydrogen as mobility fuel [10], considering it's spontaneous and highly exothermic oxidation reaction with abundantly available atmospheric oxygen.

Gas adsorption can control the dispersion of gas, thus limiting the threat of chain reaction and making the explosive gas safe to handle. Chemisorption and physisorption are the two possible means that can serve better hydrogen storage in various materials. Physisorption holds the multiple layers of gas with week Van der wall forces that can be easily reversed to generate hydrogen in less energy expense on demand. Hence it is desirous to generate the micro-porous materials with higher affinity for hydrogen physisorption [11].

Carbon nano material (CNM) provides good mechanical strength and is known to adsorb hydrogen in multiple layers. However, the cost of materials for hydrogen storage may surpass the benefits of usage of hydrogen as fuel considering economics. Hence it is desirous to generate CNMs from the renewable and inexpensive sources that have good multilayer hydrogen physisorption properties and excellent mechanical strength to withstand harsh conditions and store sufficient amount of hydrogen under pressurised conditions [12].

The hydrogen storage capacity of Nano-material of 6.5 wt% for its commercialisation as energy source is proposed by US-DOE (Department of energy). The US-DOE has directed the researcher in this field to target its vehicle storage capacity as 5.5 wt% in 2020 [13].

The current research work is motivated to generate the CNMs from plant waste, sugarcane bagasse (SCB) and its further modification for greater hydrogen physisorption for hydrogen storage. SCB was subjected to pyrolysis at elevated temperatures of 750°C to generate porous CNMs with excellent mechanical strength which was decorated with CuNPs to enhance hydrogen storage capacity of the CNM thus developed.

II. EXPERIMENTAL TECHNIQUE

A. Synthesis of CuNPs Decorated CNM

SCB was pyrolyzed in Lindberg horizontal tube furnace at 750°C in an inert atmosphere. The as-obtained carbon was further activated by treating it with alkali solutions. The activated carbon was then loaded with copper particles and annealed in the presence of carbon dioxide (CO_2) to get highly porous carbon nanomaterial which was studied for hydrogen adsorption properties using the Sievert's apparatus [16][17].

B. Hydrogen Adsorption by Sievert's Apparatus

Adsorption of hydrogen was studied by Sievert's apparatus at a pressure of 60 bars at ambient temperature using Van der Waals real gas equation [18]. 5g of CNM samples were loaded in a sample holder of Sievert's apparatus whose observations are tabulated in below Table I.

TABLE I: HYDROGEN ADSORPTION BY CNMS ANNEALED AT DIFFERENT TEMPERATURE

S. No.	CNM	Annealing Temperature	Tapped Density	Pore Volume at N_2 partial pressure of 94.99 %	Hydrogen Adsorption at 60 bar H_2 pressure and ambient temperature
		° C	g/cc	cc/g	% w/w
1	D6	600	0.1775	0.2877	4.34
2	D9	700	0.1919	0.2652	4.07

III. RESULTS AND DISCUSSIONS

A. XRD Analysis of CNMs

The CNMs were subjected to X-Rays Diffraction (XRD) analysis using Malvern Panalytical's Empyrean diffractometer having X-ray tube with Cu target of wavelength as Cu Kα-1.54184 Å and X-ray generator of 45kV & 40mA. XRD diffraction peaks were obtained in continuous scanning mode with a scanning range of Diffraction angle (2θ) as 10–90°.

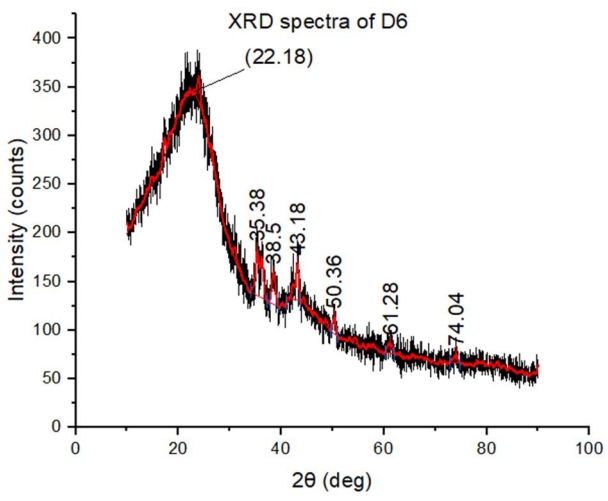

Fig. I XRD Spectra of D6

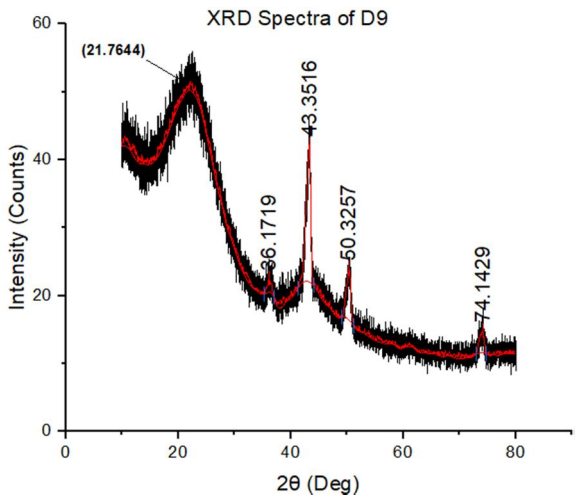

Fig. II XRD Spectra of D9

TABLE II: PEAK TABLE OF XRD ANALYSIS OF CNMs

(h,k,l) Index	Standard 2θ in deg from JCPDS: Cu file. No. 04-0836	D6			D9		
		2θ in deg	FWHM in deg	Particle Size in nm	2θ in deg	FWHM in deg	Particle Size in nm
(1, 1, 1)	43.297	43.18	0.6029	14.3	43.35	0.9613	8.7
(2, 0, 0)	50.433	50.36	0.6549	12.2	50.33	0.9097	8.7
(2, 2, 0)	74.130	74.04	0.7691	13.3	74.14	1.0056	9.8

The results are depicted in Fig. I and Fig. II and Table II. The observed values of diffraction angles are in good agreement with standard values of CuNPs in JCPDS file. No. 04-0836. Reflection Planes observed from diffraction spectra as mentioned in the Table II indicate FCC structure of copper particles [19]. From the ICDD card No. 00-056-0159, The broad humps in the spectra in the lower range at 22.18° & 21.76° diffraction angle of D6 & D9 respectively indicate amorphous phase due to reduced Graphene Oxide (rGO) with further confirmation of broad and week intensity peak at 43° diffraction angle which are deconvulated from CuNPs merging peak in both carbon material [18][19][20].

Further, Full width at half maximum (FWHM) of peak was used to calculate particle size of CuNPs for both materials using Debye Scherer's equation [18]. Particle size of CuNPs in D6 is in the range of 12.2 to 14.3 nm and that of D9 is 8.7 to 9.8 nm. It was observed that as the annealing temperature increases from 600°C to 700°C particle size of CuNPs decorated on CNMs decreases showing the annealing temperature effect. Thus XRD confirms Nano structure of the material which is further explored in SEM analysis.

B. SEM Analysis of CNMs

Scanning Electron Microscopy (SEM) provides crucial information regarding the morphology of the microstructures of the CNMs. These CNMs synthesised from SCB were subjected to SEM analysis using FEI Quanta 200 FEG SEM for elucidating the surface morphology and its correlation to annealing temperature. Fig. III shows spherical beads of CuNPs of size of 30-40 nm range decorated over the porous structure of CNMs in D6 sample while that of D9 in Fig. IV, the particle size of 20-30 nm observed thus showing the temperature effect.

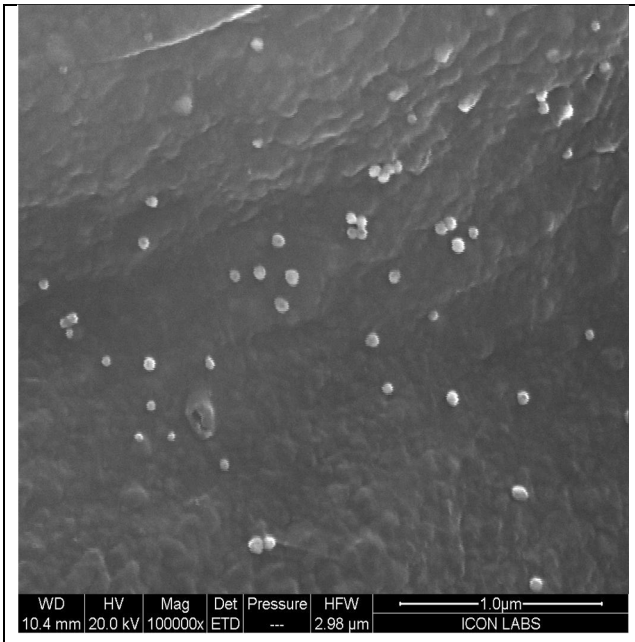

Fig. III SEM Image of D6

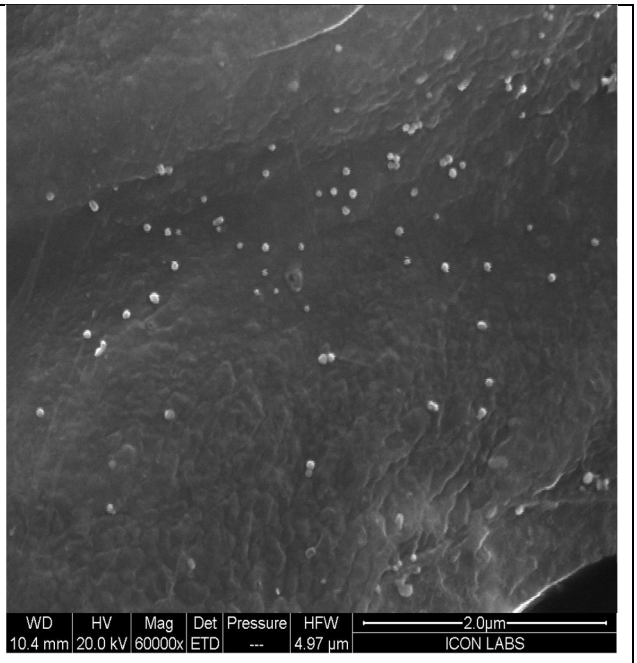

Fig. IV SEM Image of D9

C. ICP-AES analysis of CNMs for Copper deposited concentration throughout the bulk

Inductively Coupled Plasma - Atomic Emission Spectroscopy (ICP-AES) analysis of CNMs was conducted for estimating amount of Copper deposited on CNMs. Around 0.1g of CNMs was digested for 10 minutes in 10ml of 1:1 HCL in water from Millipore. HCl reagent was used of analytical grade. The remains further extracted with Millipore water, filtered and filtrate further diluted in 100mL Millipore water. Diluted solutions were aspirated in ARCOS ICP spectrometer of RF generator of 1.6 kW, 27.12 MHz and wavelength range of 130-770 nm with resolution of 9 picometer. Results obtained were tabulated in below Table III.

Table III Copper Concentration of CNMs by ICP-AES

Sample	Percentage of Copper in CNMs
D6	2.442
D9	2.337

D. EDAX Analysis of CNMs

Energy Dispersive X-Ray (EDAX) Analysis of CNMs using FEI Quanta 200 FEG SEM gave surface concentration of CuNPs around 2.8% with overall uncertainty of 9.87%. Major elements Carbon being 89.7 % and Oxygen is 7.2 % are indicated in the EDAX spectra in below figure. Rest other minor elements is neglected considering the uncertainty of analysis.

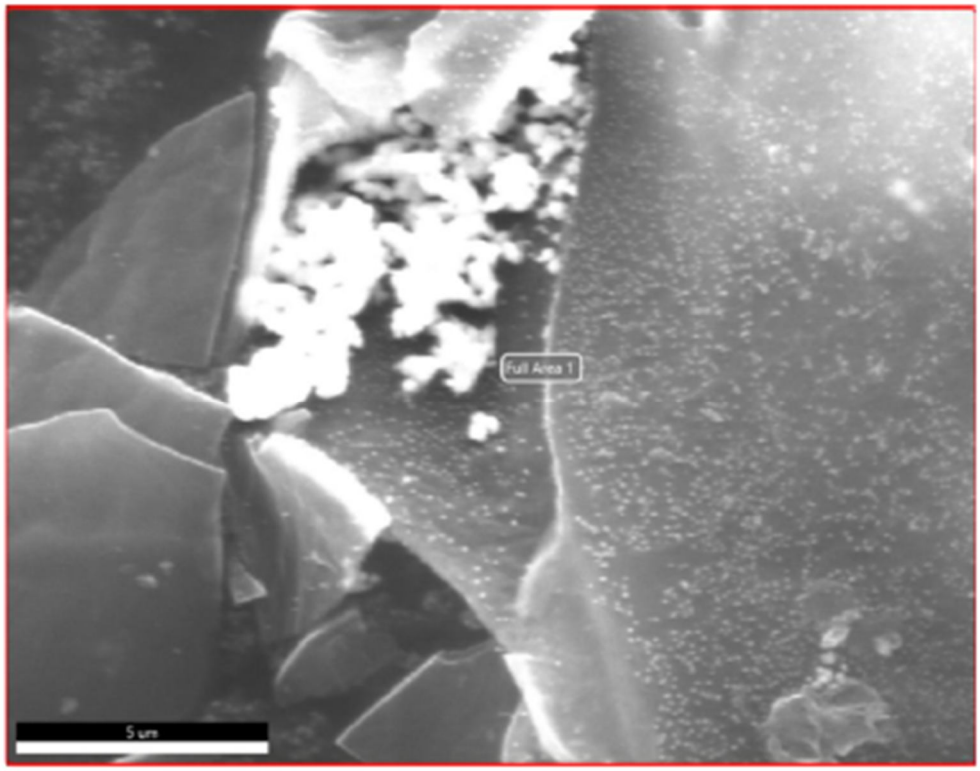

Fig. V Surface Area in SEM image covered for EDAX

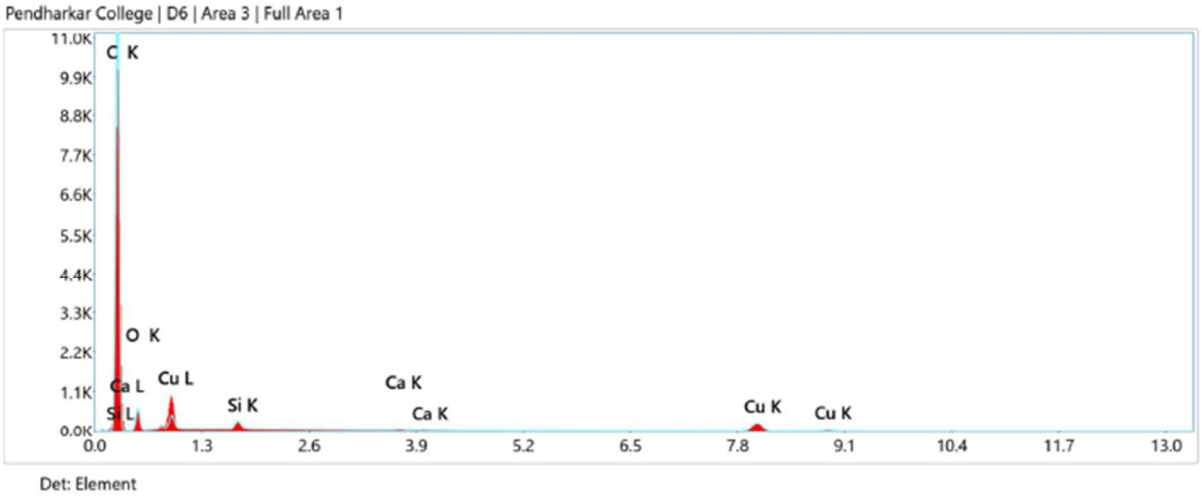

eZAF Quant Result - Analysis Uncertainty: 9.41 %

Element	Weight %	MDL	Atomic %	Net Int.	Error %	R	A	F
C K	89.7	0.04	93.7	2103.1	9.2	0.9384	0.2112	1.0000
O K	7.2	0.18	5.6	112.9	13.4	0.9460	0.0554	1.0000
Si K	0.3	0.03	0.1	58.6	10.1	0.9619	0.7373	1.0058
Ca K	0.1	0.05	0.0	6.6	56.1	0.9732	0.9690	1.0501
Cu K	2.8	0.11	0.6	111.6	5.5	0.9864	0.9964	1.1771

Fig. VI EDAX Spectra with Result table

E. Raman Spectroscopic Analysis of CNMs

Raman Spectroscopic Analysis of CNMs was carried out using Invia Reflex Raman Spectrometer of Renishaw with Excitation source of Laser HeNe of wavelength 633 nm and Power 17 mW capable of producing Raman wavenumber transfer 50 to 4000 cm^{-1} of Spectral Range of 200 nm – 1600 nm.

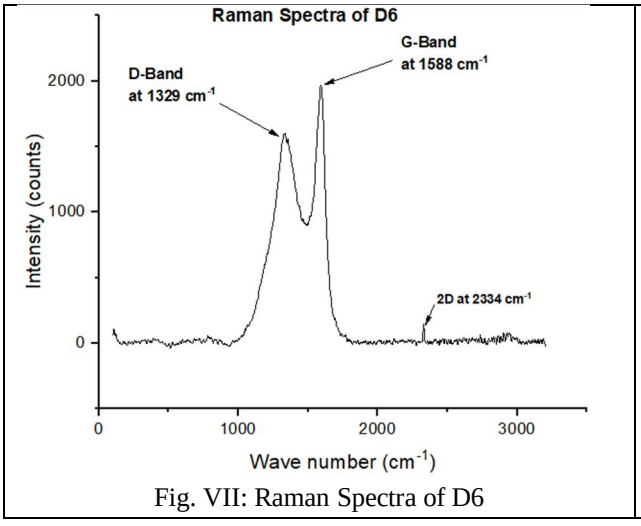

Fig. VII: Raman Spectra of D6

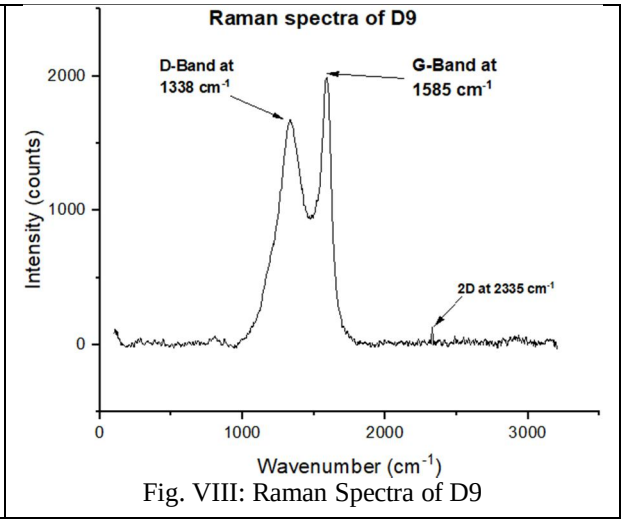

Fig. VIII: Raman Spectra of D9

TABLE IV: PEAK TABLE OF RAMAN ANALYSIS OF CNMs

Parameters	D6			D9		
	Peak-1 D-Band at 1329 cm^{-1}	**Peak-2 G-Band at 1588 cm^{-1}**	**Ratio 0f I_D/I_G**	**Peak-1 D-Band at 1338 cm^{-1}**	**Peak-2 G-Band at 1585 cm^{-1}**	**Ratio 0f I_D/I_G**
Intensity	1603	1969	0.81	1672	1980	0.84
Area	274394	338099	0.81	160927	191981	0.84

Raman spectroscopic analysis results of both the material in above Fig. VII, Fig. VIII and Table IV elucidates two peaks at around 1329cm^{-1} and 1585cm^{-1} as D-band and G-band belonging to mixture of Distorted and graphitic sp^2 carbon whose intensity and area ratio calculated as 0.81 for D6 and 0.84 for D9 confirms that the distorted sp^2 carbon increases with the increase in annealing temperature during synthesis of CNMs from SCB [13][22]. Less intense Peak at 2334cm^{-1} and 2335cm^{-1} in D6 & D9 spectra respectively represents 2D band as a overtones of D band of sp^2 graphitic carbon [23].

IV. CONCLUSION

From all the above analysis, it can be concluded that with the increase in annealing temperature, I_D/I_G ratio of Raman spectra increases, indicating the increase in the defects in graphitic carbon while copper deposition on the porous carbon decreases along with the decrease of copper particle size. Pore Volume of CNM too decreases and hence hydrogen adsorption capacity decreases with increase in annealing temperature for the synthesis of CNMs from SCB. Decrease in hydrogen adsorption with decrease in copper deposition co-relates with the spill over effect of CuNPs [24] [25].

V. ACKNOWLEDGEMENT

We sincerely express our gratitude to ICON LAB (Mumbai), SAIF (IIT Bombay) and SMART Instrument LAB (Thane) for carrying out the analysis and characterization of synthesized CNMs.

REFERENCES

[1] Cheng, H. M., Yang, Q. H., & Liu, C. (2001). Hydrogen storage in carbon nanotubes. Carbon, 39(10), 1447–1454. https://doi.org/10.1016/S0008-6223(00)00306-7
[2] Rosen, M. A. (2015). The Prospects for Renewable Energy through Hydrogen Energy Systems. Journal of Power and Energy Engineering, 03(04), 373–377. https://doi.org/10.4236/jpee.2015.34050
[3] Chen, P., & Zhu, M. (2008). Recent progress in hydrogen storage. In Materials Today (Vol. 11, Issue 12, pp. 36–43). https://doi.org/10.1016/S1369-7021(08)70251-7
[4] Yang, S. J., Jung, H., Kim, T., & Park, C. R. (2012). Recent advances in hydrogen storage technologies based on nanoporous carbon materials. Progress in Natural Science: Materials International, 22(6), 631–638. https://doi.org/10.1016/j.pnsc.2012.11.006
[5] Rajalakshmi, * N, Sarada, B. Y., & Dhathathreyan, K. S. (2015). Porous Carbon Nanomaterial from Corncob as Hydrogen Storage material. In Agricultural Science Research Journal (Vol. 5, Issue 2). http://www.resjournals.com/ARJ
[6] Mao, S. S., Shen, S., & Guo, L. (2012). Nanomaterials for renewable hydrogen production, storage and utilization. In Progress in Natural Science: Materials International (Vol. 22, Issue 6, pp. 522–534). Elsevier B.V. https://doi.org/10.1016/j.pnsc.2012.12.003
[7] Poullikkas, A., & Nikolaidis, P. (n.d.). (2017) A comparative review of electrical energy storage systems for better sustainability. Journal of Power Technologies 97 (3) (2017) 220-245 https://www.researchgate.net/publication/320755664
[8] Puszkiel, J., Garroni, S., Milanese, C., Gennari, F., Klassen, T., Dornheim, M., & Pistidda, C. (2017). Tetrahydroborates: Development and potential as hydrogen storage medium. In Inorganics (Vol. 5, Issue 4). MDPI Multidisciplinary Digital Publishing Institute. https://doi.org/10.3390/inorganics5040074
[9] Young, K. hsiung, & Nei, J. (2013). The current status of hydrogen storage alloy development for electrochemical applications. Materials, 6(10), 4574–4608. https://doi.org/10.3390/ma6104574
[10] Yang, S. J., Jung, H., Kim, T., & Park, C. R. (2012). Recent advances in hydrogen storage technologies based on nanoporous carbon materials. Progress in Natural Science: Materials International, 22(6), 631–638. https://doi.org/10.1016/j.pnsc.2012.11.006
[11] Züttel, A. (2003). Materials for hydrogen storage.
[12] Panella, B., Hirscher, M., & Roth, S. (2005). Hydrogen adsorption in different carbon nanostructures. Carbon, 43(10), 2209–2214. https://doi.org/10.1016/j.carbon.2005.03.037
[13] Ariharan, A., Viswanathan, B., & Nandhakumar, V. (2017). Nitrogen Doped Graphene as Potential Material for Hydrogen Storage. Graphene, 06(02), 41–60. https://doi.org/10.4236/graphene.2017.620042
[14] Jaguaribe, E. F., Medeiros, L. L., Barreto, M. C. S., & Araujo, L. P. (n.d.). THE PERFORMANCE OF ACTIVATED CARBONS FROM SUGARCANE BAGASSE, BABASSU, AND COCONUT SHELLS IN REMOVING RESIDUAL CHLORINE. 22(01), 41–47. www.abeq.org.br/bjche

[15] Mohamed, E. F., El-Hashemy, M. A., Abdel-Latif, N. M., & Shetaya, W. H. (2015). Production of sugarcane bagasse-based activated carbon for formaldehyde gas removal from potted plants exposure chamber. Journal of the Air and Waste Management Association, 65(12), 1413–1420. https://doi.org/10.1080/10962247.2015.1100141
[16] Sharon, M., Sharon, M., Kalita, G., & Mukherjee, B. (2011). Hydrogen Storage by Carbon Fibers Synthesized by Pyrolysis of Cotton Fibers. Carbon Letters, 12(1), 39–43. https://doi.org/10.5714/cl.2011.12.1.039
[17] Mukherjee, B., Sharon, M., Kalita, G., & Sharon, M. (2016). Ambiguity in determining H2 adsorption capacity of carbon fiber by pressure technique. International Journal of Hydrogen Energy, 41(4), 2671–2676. https://doi.org/10.1016/j.ijhydene.2015.12.110
[18] Mukherjee, B., Kalita, G., Sharon, M., & Sharon, M. (2013). Hydrogen storage by carbon fibers from cotton. QScience Connect, 2013, 45. https://doi.org/10.5339/connect.2013.45
[19] B.D.Cullity, “Elements of X-ray Diffraction”, Addison-Wesley Pub.Co., (1978).
[20] Astuti, F., Sari, N., Maghfirohtuzzoimah, V. L., Asih, R., Baqiya, M. A., & Darminto, D. (2020). Study of the formation of amorphous carbon and rGO-like phases from palmyra sugar by variation of calcination temperature. Jurnal Fisika Dan Aplikasinya, 16(2), 91. httpsdoi.org10.12962j24604682.v16i2.6706
[21] Mukherjee, Dr. B. T., & Sainik, Shyambabu. K. (2022). Taguchi Optimization Methodology Directed Synthesis of CNMs from Plant Fibres Decorated with Metal Nano Particles for Study of Microwave Absorption in S and C Bands. International Journal of Recent Technology and Engineering (IJRTE), 11(3), 66–77. httpsdoi.org10.35940ijrte.C7263.0911322
[22] Muhammad Hafiz, S., Ritikos, R., Whitcher, T. J., Md. Razib, N., Bien, D. C. S., Chanlek, N., Nakajima, H., Saisopa, T., Songsiriritthigul, P., Huang, N. M., & Rahman, S. A. (2014). A practical carbon dioxide gas sensor using room-temperature hydrogen plasma reduced graphene oxide. Sensors and Actuators, B Chemical, 193, 692–700. httpsdoi.org10.1016j.snb.2013.12.017
[23] Hodkiewicz, J. (n.d.). Characterizing Graphene with Raman Spectroscopy. Thermo Scientific. Application Note 51946.
[24] Takagi, H., Hatori, H., & Yamada, Y. (2004). Hydrogen adsorption/desorption property of activated carbon loaded with platinum. Chemistry Letters, 33(9), 1220–1221. https://doi.org/10.1246/cl.2004.1220.
[25] Konda, S. K., & Chen, A. (2016). Palladium based nanomaterials for enhanced hydrogen spillover and storage. In Materials Today (Vol. 19, Issue 2, pp. 100–108). Elsevier. https://doi.org/10.1016/j.mattod.2015.08.002

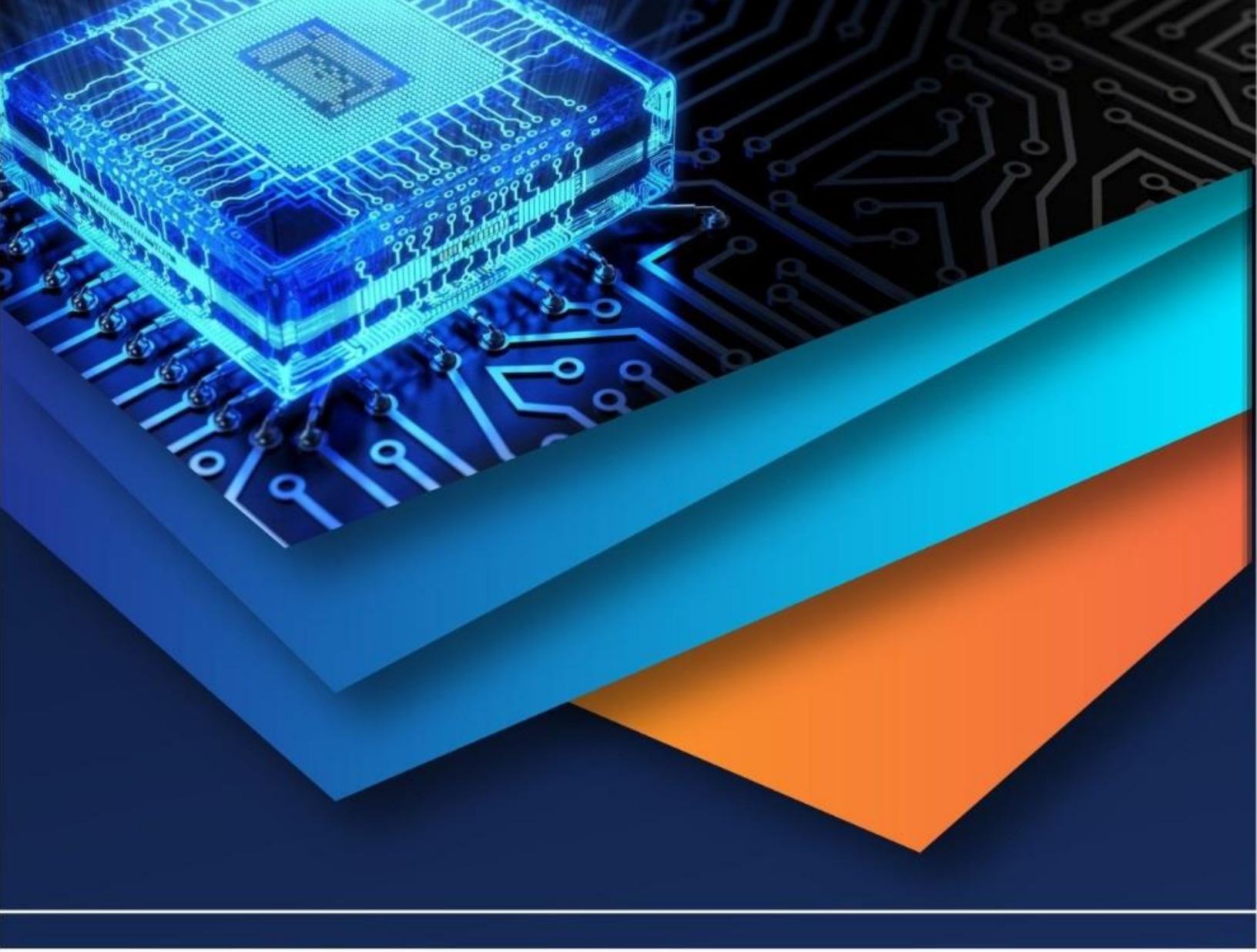

10.22214/IJRASET

45.98

IMPACT FACTOR: 7.129

IMPACT FACTOR: 7.429

INTERNATIONAL JOURNAL FOR RESEARCH

IN APPLIED SCIENCE & ENGINEERING TECHNOLOGY